ELSEVIER

Journal of Fluids and Structures 25 (2009) 742–750

JOURNAL OF FLUIDS AND STRUCTURES

www.elsevier.com/locate/jfs

Experimental investigation of Vortex-Induced Vibration on rigid, smooth and inclined cylinders

G.R. Franzini[a,*], A.L.C. Fujarra[b], J.R. Meneghini[a], I. Korkischko[a], R. Franciss[c]

[a]*NDF, POLI, University of São Paulo, Brazil*
[b]*Department of Naval Architecture and Ocean Engineering, POLI, University of São Paulo, Brazil*
[c]*CENPES, Petrobras, Rio de Janeiro, Brazil*

Received 1 May 2008; accepted 16 January 2009
Available online 12 March 2009

Abstract

This paper presents new experimental results of Vortex-Induced Vibration (VIV) on inclined cylinders. Models are mounted on a low damping air-bearing elastic base with one degree-of-freedom, constrained to oscillate only in the transverse direction to a free stream. The Reynolds number varied in the range $2000 \lesssim Re \lesssim 8000$. New measurements on the dynamic response oscillations of inclined cylinders, due to VIV, are compared with previous experiments of a vertical cylinder. Models with circular and elliptical cross sections have been tested. The purpose of this work is to check the validity of the normal velocity correction of VIV studies of inclined structures. The results show that the reduced velocity range, in which the upper and lower branches of VIV occurs, is similar to the vertical cylinder case if the proper projected velocity is considered. Tests have been conducted to support this observation with inclinations up to 45°. We have also observed that the amplitudes of oscillation of the inclined circular cylinder are comparable, but slightly lower than, to the amplitudes observed in the vertical cylinder experiments. Measured forces and added mass also show similar behaviour. However, for cases with an elliptical cylinder, the amplitudes of oscillation are considerably lower than those observed for a circular cylinder. This difference is explained by the higher added mass of the elliptical cylinder.

Keywords: Vortex-Induced Vibration; Flow around inclined cylinders; Bluff body

1. Introduction

Long risers are used in the exploration of petroleum and natural gas, and they are hanged in catenary from platforms to the seabed. The flow around these structures are subject to vortex shedding, an unsteady phenomenon that modifies the pressure field on the risers' surface, causing an oscillatory force that acts in the riser. If the vortex shedding frequency is close to one of the natural frequencies of oscillation, the structure can oscillate at high amplitudes. Such kind of oscillation is usually known as Vortex-Induced Vibration (VIV). The papers written by Sarpkaya (1979), Parkinson (1989), Bearman (1984) and Williamson and Govardhan (2004) are excellent surveys on the subject.

*Corresponding author. Tel.: +55 11 3091 5724; fax: +55 11 3091 5642.
E-mail address: guilherme.franzini@gmail.com (G.R. Franzini).

0889-9746/$ - see front matter © 2009 Elsevier Ltd. All rights reserved.
doi:10.1016/j.jfluidstructs.2009.01.003

VIV is a self-regulated and self-excited phenomenon, so it can lead to fatigue failure. Most of the algorithms of fatigue analysis of risers subjected to VIV considers that the flow around an inclined cylinder can be considered equivalent to the one in which the free stream velocity is projected on to the direction orthogonal to the cylinder axis [see Yamamoto et al. (2004) and Meneghini et al. (2004)]. In the present work, this simplification is referred as the normal velocity correction to VIV on inclined cylinders. The main objective of this paper is to check and discuss the validity of such approximation.

We can remark two experimental investigations concerning VIV problem in which the flow is not normal to the cylinder axis. Ramberg (1983) presents results for forced oscillations and at a lower Reynolds number range (160–1000). Yttervik et al. (2003) studied long flexible cylinders immersed in currents at large experimental facilities. A numerical study of the flow around a curved cylinder and its three dimensionalities effects on the wake pattern were carried out by Miliou et al. (2007).

This paper presents new measurements of VIV of inclined cylinders, in a Reynolds number range between $\mathrm{Re} \approx 2000$ and 8000. The experiments have been carried out in a very well controlled experimental facility. In order to check the validity of the normal velocity correction, the present investigation has been carried out testing a rigid cylinder mounted on an low damping elastic base, inclined in relation to the vertical by an angle $\theta = 20^\circ$ and 45°. The results for these configurations are compared with those of a cylinder vertically mounted on the elastic base. The influence of the immersed length is also discussed.

2. Experimental arrangement

Tests were conducted at the Fluid-Dynamics Research Group Laboratory (NDF) of the University of São Paulo (USP). The circulating water channel facility had $(0.70 \times 0.80 \times 7.50)$ m test section. This channel operates at a low turbulence level ($<2\%$), and can operate at good quality and well controlled flows up to 0.7 m/s. Rigid cylinder models were made of plexiglas with diameter $D = 32$ mm and wet-length $L = 585$ and 773 mm. In all experiments, the mass parameter ($m^* = 4m/\pi\rho D^2 L$, where m is the moving system mass) was kept constant and equal to approximately 2.5. This mass parameter is defined as the ratio of the mass of moving parts by the displaced mass of water. Cylinders were vertically clamped by their upper end at an air-bearing elastic base fixed on the channel structure and terminated at their lower end with a 3.0 mm gap on to the test section floor. The lower ends of the models were parallel to the channel floor.

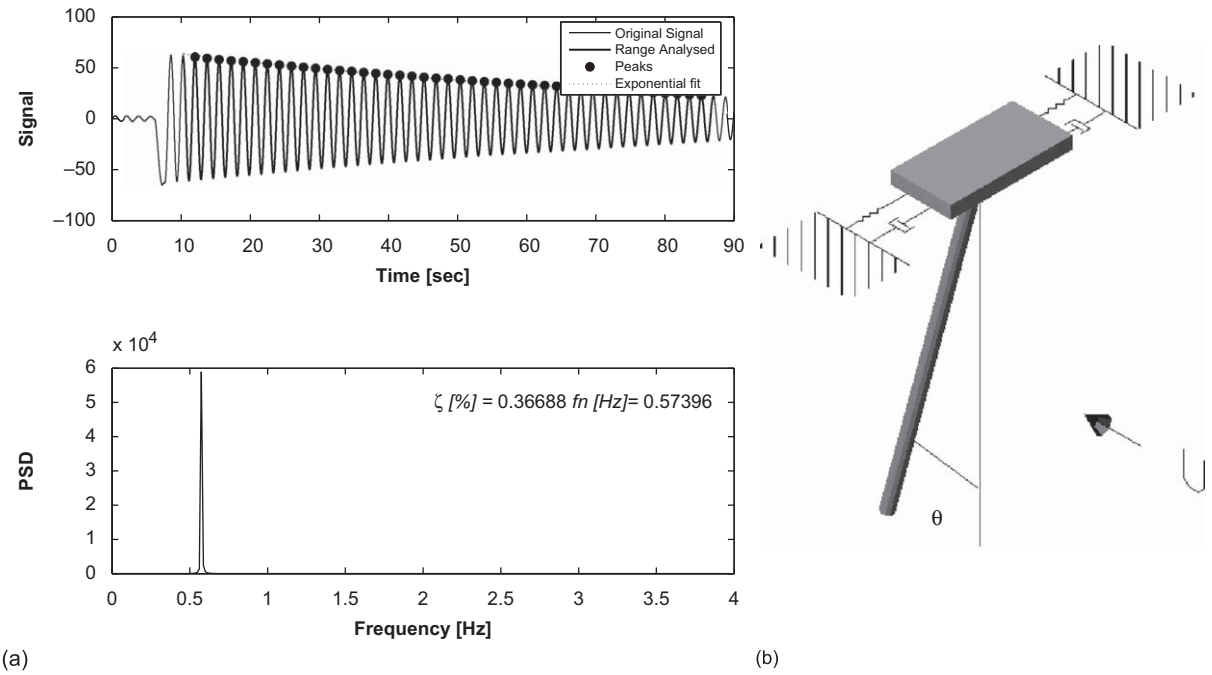

Fig. 1. Typical free decay results and experimental set up. (a) Decay test in air; (b) inclined cylinder configuration and elastic base outline.

The base had a very low structural damping coefficient ($\zeta \approx 0.5\%$), leading to a mass-damping parameter $m^*\zeta = 0.0125$. The open section channel facility was equipped with glass walls and floor, offering a complete view of the models. Further details regarding the circulating water channel can be found in Assi et al. (2006).

Forces were measured using an ATI (NANO25) load cell fixed on the model, and the crosswise vibration was measured employing a LEUZE (ODSL 8/V4 model) laser position sensor. Fig. 1(a) shows a typical decay test result in air, and Fig. 1(b) shows the experimental set up for the inclined cylinder tests.

Three sets of experiments were conducted, with the cylinder free to oscillate only transversely to flow direction. In the first set, vertical cylinders with maximum immersed lengths $L = 585$ and 773 mm were tested. Two different immersed lengths were employed in order to check the influence of this length on the response. As the results showed no discernable difference, the shorter cylinder was employed. This condition is referred to as the vertical condition, and all the other results were then compared to this case.

In the second set of experiments, the circular cylinder was mounted not vertically but inclined in relation to the vertical. For both inclinations, the immersed length was kept constant and equal to 585 mm. The amplitude and frequency of oscillation versus reduced velocity, together with drag and lift coefficients were obtained and compared to the vertical cylinder condition.

In the third set of experiments, an elliptical cylinder, with immersed length 585 mm, was investigated. The cross section area of this elliptical cylinder is made equal to the intersection area of an horizontal plane with the circular cylinder inclined by an angle $\theta = 45^\circ$.

3. Results and discussion

The dynamic responses of the models are described in terms of the nondimensional amplitude A/D versus the reduced velocity $V_r = U/f_nD$. The natural frequency (f_n) was obtained for each case from decaying tests in water.

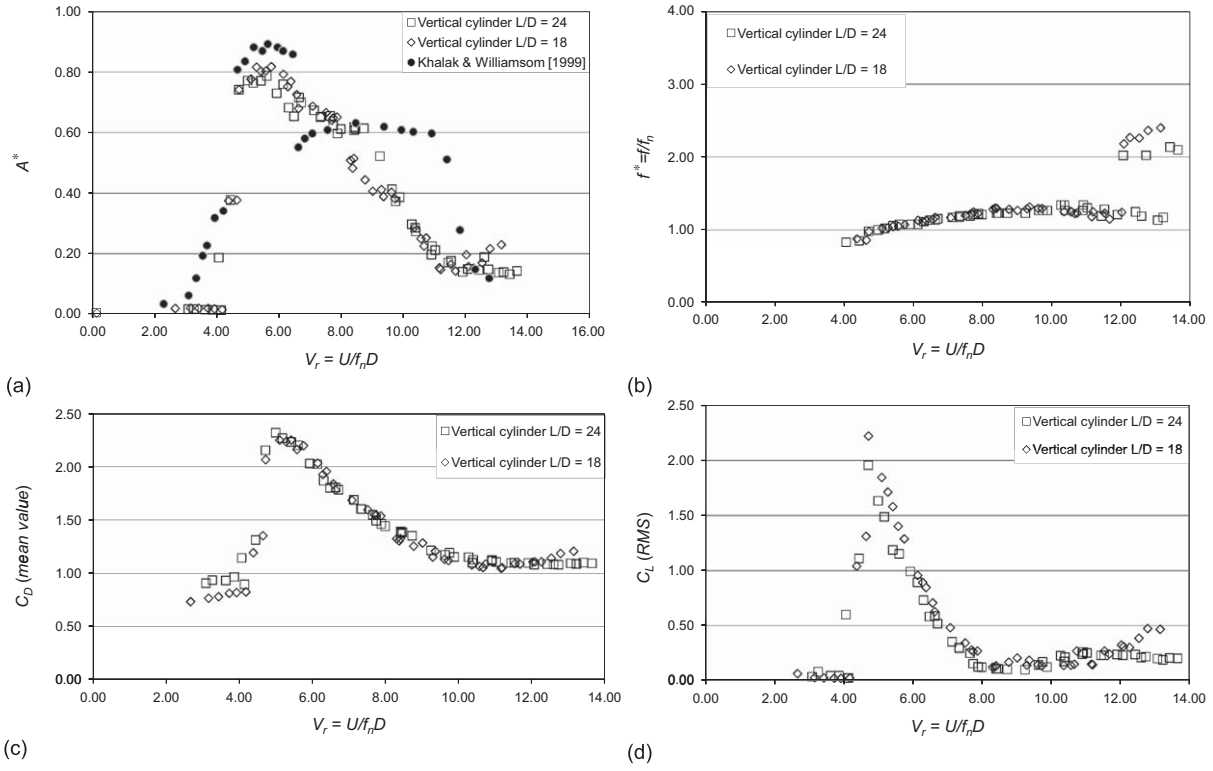

Fig. 2. Free oscillation of a vertical circular cylinder mounted on an elastic base and immersed lengths $L = 773$ and 585 mm. (a) Amplitude of oscillation A^*; (b) normalised frequency response f^*; (c) mean drag coefficient C_D; (d) r.m.s. of lift coefficient $C_{L_{\text{rms}}}$.

The plot of the reduced frequency f/f_n versus V_r was also obtained (f is the oscillation frequency). Amplitudes were calculated by taking the average of the 10% highest peaks recorded on the time history of displacement. Reynolds number (calculated with diameter D and flow velocity U) range from Re $\approx$ 2000 to 8000 in all experiment cases. The reduced velocity V_r range extended to a maximum value of 14 for all tested cases.

3.1. First set of experiments: vertical circular cylinder

In the first set of experiments, a vertical circular cylinder was tested in the range of reduced velocity $3 < V_r < 14$. This range is large enough to identify the lock-in region, where the higher amplitudes are observed.

In order to analyse the influence of the immersed length on the results, two cylinders have been tested, one with an immersed length $L = 773$ mm and the other with $L = 585$ mm. These two cases have aspect ratios $L/D \approx 24$ and 18, respectively. In both, the cylinder mass parameter was kept approximately constant ($m^* \approx 2.5$). A free-decay test in water has been carried out and the natural frequency $f_n = 0.48$ Hz was obtained from this test. The reduced velocity was calculated with this natural frequency. The results of amplitude of oscillation for these vertical cylinders are shown in Fig. 2(a), together with those measured by Khalak and Williamson (1999). As one can observe in this figure, the maximum amplitude is very close to the one measured by Khalak and Williamson (1999). This small difference can be explained considering that the parameters from both experiments are not exactly the same. Also, one can notice that the lower branch in our experiments, employing the classification proposed by Khalak and Williamson (1999), is shorter and the amplitude drops more steeply. Probably, the differences of both experiments in the parameters are the cause of such disagreement. However, in the present experimental results it is possible to notice a small range of V_r in which the amplitude of oscillation is approximately $0.6D$, the same value of amplitude observed in Khalak and Williamson (1999) in the lower branch.

The amplitude of oscillation is shown in Fig. 2(a), the normalised frequency response (f^*) in Fig. 2(b), the mean drag coefficient (C_D) in Fig. 2(c), and the rms of lift coefficient ($C_{L_{\text{rms}}}$) in Fig. 2(d). As we can see analysing these figures, there are no noticeable differences among the results obtained with vertical cylinders with those two immersed lengths.

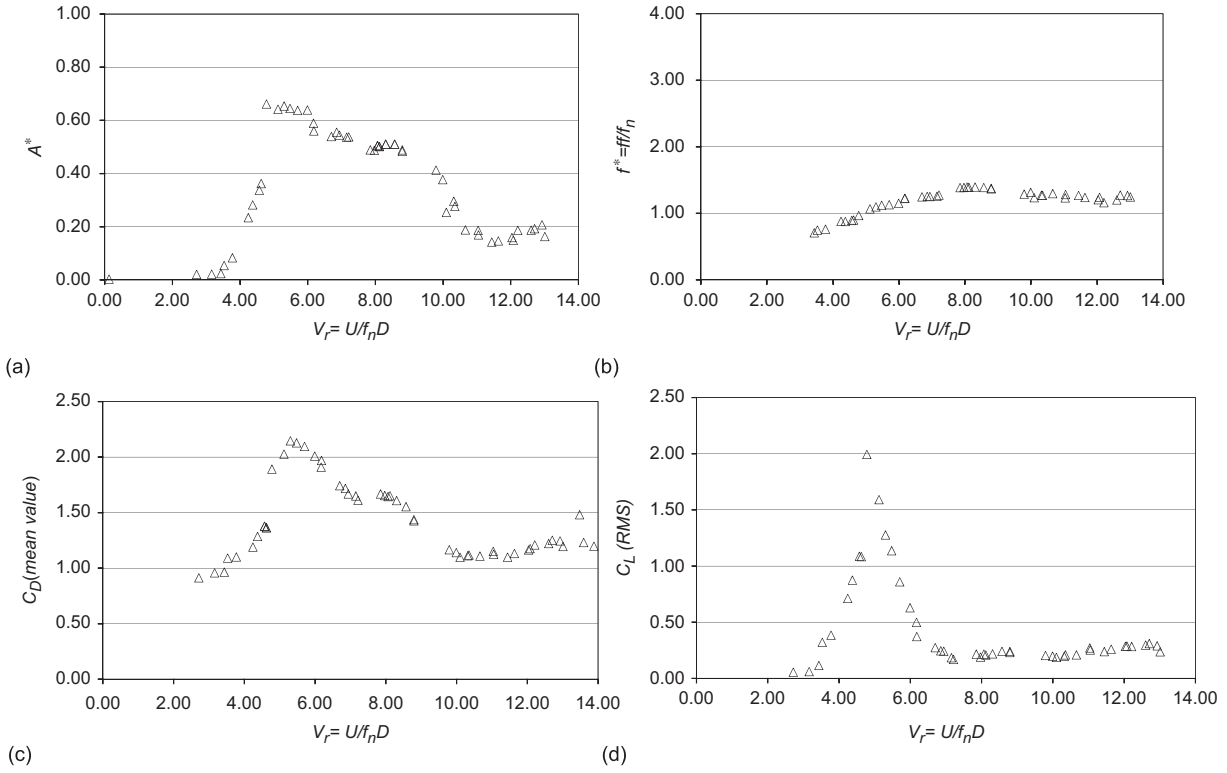

Fig. 3. Free oscillation of a circular cylinder, inclined at 20°, and mounted on an elastic base. (a) Amplitude of oscillation A^*; (b) normalised frequency response f^*; (c) mean drag coefficient C_D; (d) r.m.s. of lift coefficient $C_{L_{\text{rms}}}$.

The case with an immersed length $L = 585\,\text{mm}$ has been chosen to be compared with the inclined circular cylinder (second set of experiments) and the elliptical cylinder results (third set of experiments).

As it can be seen in Fig. 2, the observed peak of nondimensional amplitude ($A^* = A/D$) is about 0.80 and it occurs for reduced velocity V_r close to 5.6. For each value of V_r, the time series of movement was recorded and the value of nondimensional amplitude was calculated through the mean of the 10% highest peaks of the signal. Using the modified Griffin plot, see Govardhan and Williamson (2006), for a mass ratio $m^* = 2.5$ and structural damping $\zeta = 0.5\%$, the peak of nondimensional amplitude is 0.84 which is very close to the observed value of maximum amplitudes of our experiments with this vertical cylinder. The plot of frequency ratio f^* has the same shape as the one presented in Khalak and Williamson (1999) for a similar value of m^*. The peaks of drag and lift coefficients occur at the same reduced velocity as the peak of A^*, reaching the values $C_D = 2.3$ and $C_L = 1.9$. It is possible to see the "sharp shape" of the C_L plot and the asymptote value 1.2 of the drag coefficient for $V_r > 10$. So, the results of our first set of experiments agree very well with those found in the literature. Due this fact, these results consist of a reliable data set for comparison with the ones obtained from the other sets of experiments.

3.2. Second set of experiments: inclined circular cylinder

In the second set of experiments, the circular cylinder was mounted inclined in relation to the vertical axis. Two angles θ have been tested: $\theta = 20^\circ$ and 45°. Both test conditions had immersed lengths $L = 585\,\text{mm}$, leading to an aspect ratio $L/D = 18$. The lower edge of the cylinder was parallel to the channel floor.

The results for the condition with $\theta = 20^\circ$ are shown in the Fig. 3. The maximum value of A^* is slightly below 0.70 and occurs at $V_r \approx 5-6$, as can be seen in Fig. 3(a). The value of maximum lift coefficient occurs at the same value of reduced velocity (Fig. 3(d)). Fig. 3(c) shows that the maximum value of drag coefficient is slightly lower than the one measured in the vertical cylinder case.

For the condition with $\theta = 45^\circ$, the maximum value of A^* is close to 0.70, as can be seen in Fig. 4(a). Analysing Figs. 4(c) and (d), we also observed a significant reduction on the maximum value of lift and drag coefficients. As it will

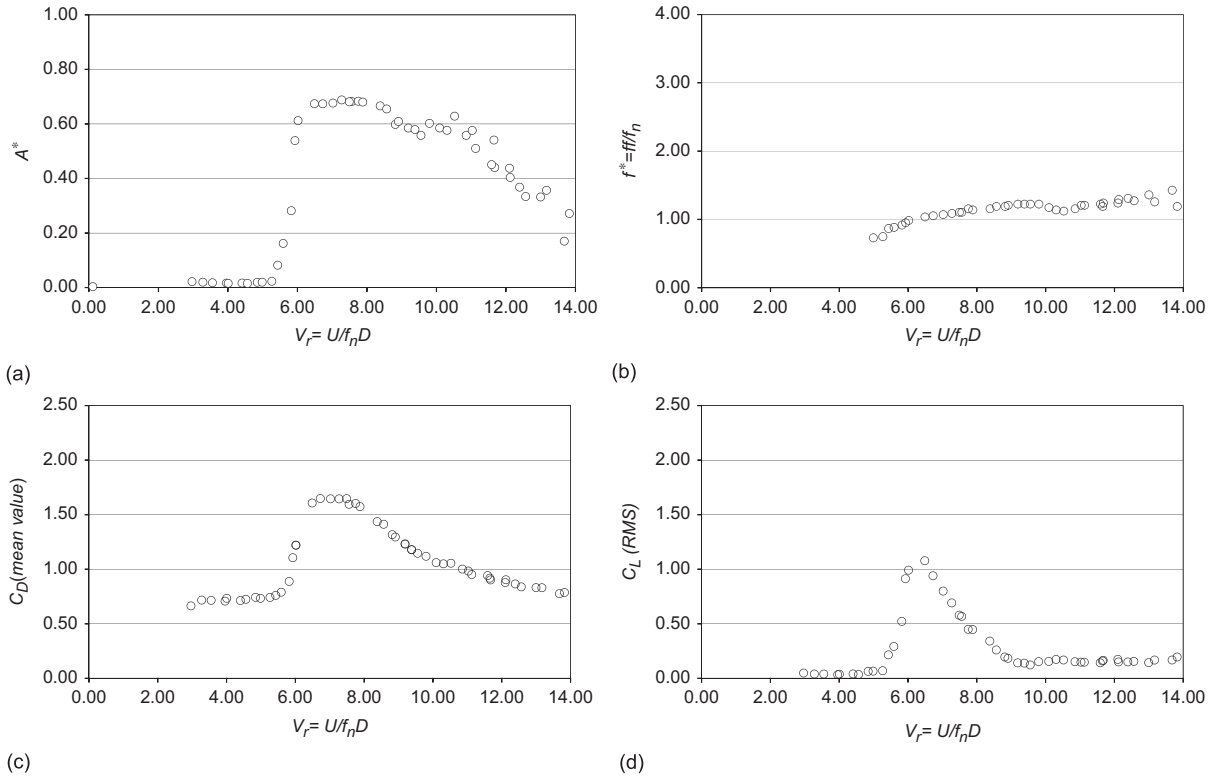

Fig. 4. Free oscillation of a circular cylinder, inclined at 45°, and mounted on an elastic base. (a) Amplitude of oscillation A^*; (b) normalised frequency response f^*; (c) mean drag coefficient C_D; (d) r.m.s. of lift coefficient $C_{L_{\text{rms}}}$.

be shown in (4), C_L results collapse to similar curves if the proper projected velocity is employed for the evaluation of the force coefficients.

3.3. Third set of experiments: a vertical elliptical cylinder

In the third set of experiments, a vertical cylinder with elliptical cross section was tested. The cross section area was made equal to the intersection area of a horizontal plane with the circular cylinder inclined by an angle $\theta = 45^\circ$. The immersed length of the model was kept at $L = 585$ mm. The purpose of this set of experiments is to check the differences between the dynamics of an inclined circular cylinder, with the free stream acting over an apparent elliptical cross section, and a vertical cylinder with the same elliptical cross area.

Analysing Fig. 5(a), one can notice that the response curve of A^* shows three well-defined branches. The first one starts at $V_r \approx 3.7$ and ends at $V_r \approx 6.5$ and represents the cylinder with no or very low amplitudes of oscillation. The second branch is in the range $4 < V_r < 12$ and the amplitude varies from 0.40 to 0.57. The last branch occurs for V_r in the range from 12 to 17, and consist in a region with values of A^* almost constant and close to 0.12.

4. Comparison of vertical and inclined cylinder results

In order to check the validity of the classical approach of VIV on inclined cylinders, the results from the three sets of experiments are compared by evaluating the reduced velocity with the component of the freestream in the normal direction to the cylinder axis. The normal reduced velocity to the cylinder axis is given by

$$V_{r,n} = \frac{U \cos\theta}{f_n D}. \tag{1}$$

The results for all cases with the effective reduced velocity evaluated in this way are shown in Fig. 6. Analysing Fig. 6(a), we can notice that the maximum value of A^* observed in the first set of experiments is slightly higher than those

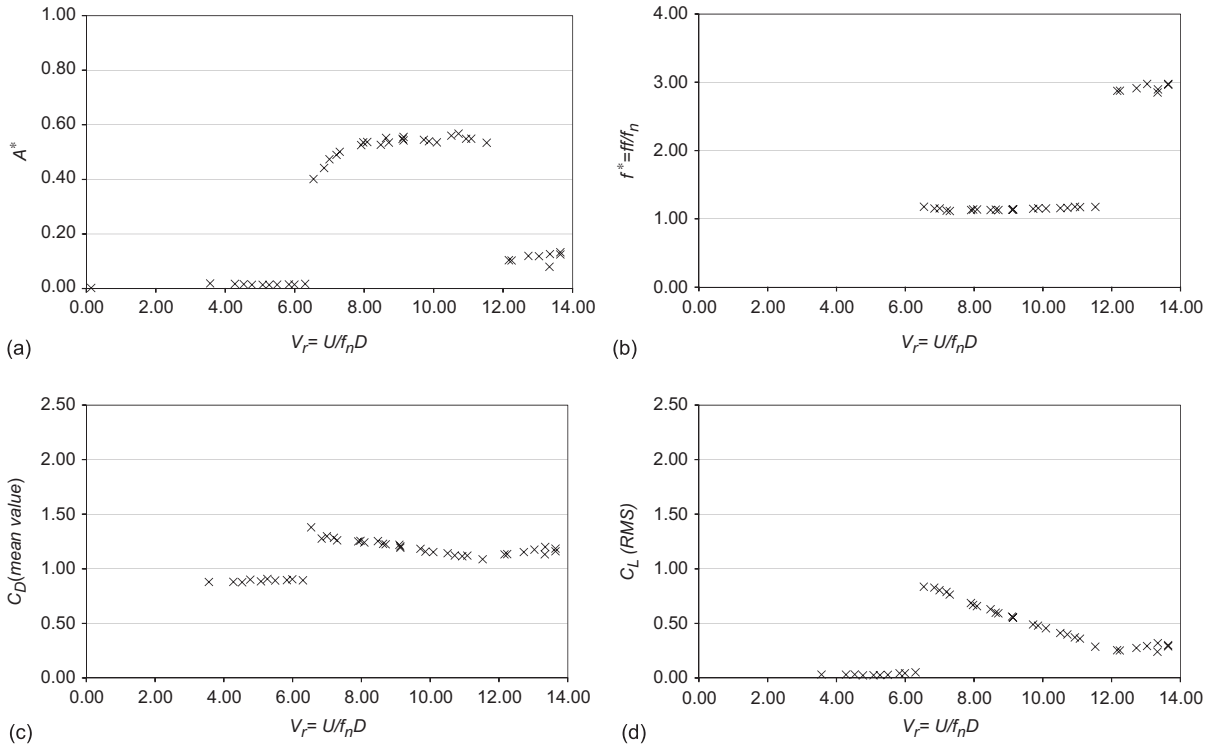

Fig. 5. Free oscillation of an elliptical cylinder mounted on an elastic base. (a) Amplitude of oscillation A^* versus the reduced velocity V_r; (b) frequency response through the synchronisation regime; (c) mean drag coefficient C_D; (d) r.m.s. of lift coefficient $C_{L_{\mathrm{rms}}}$.

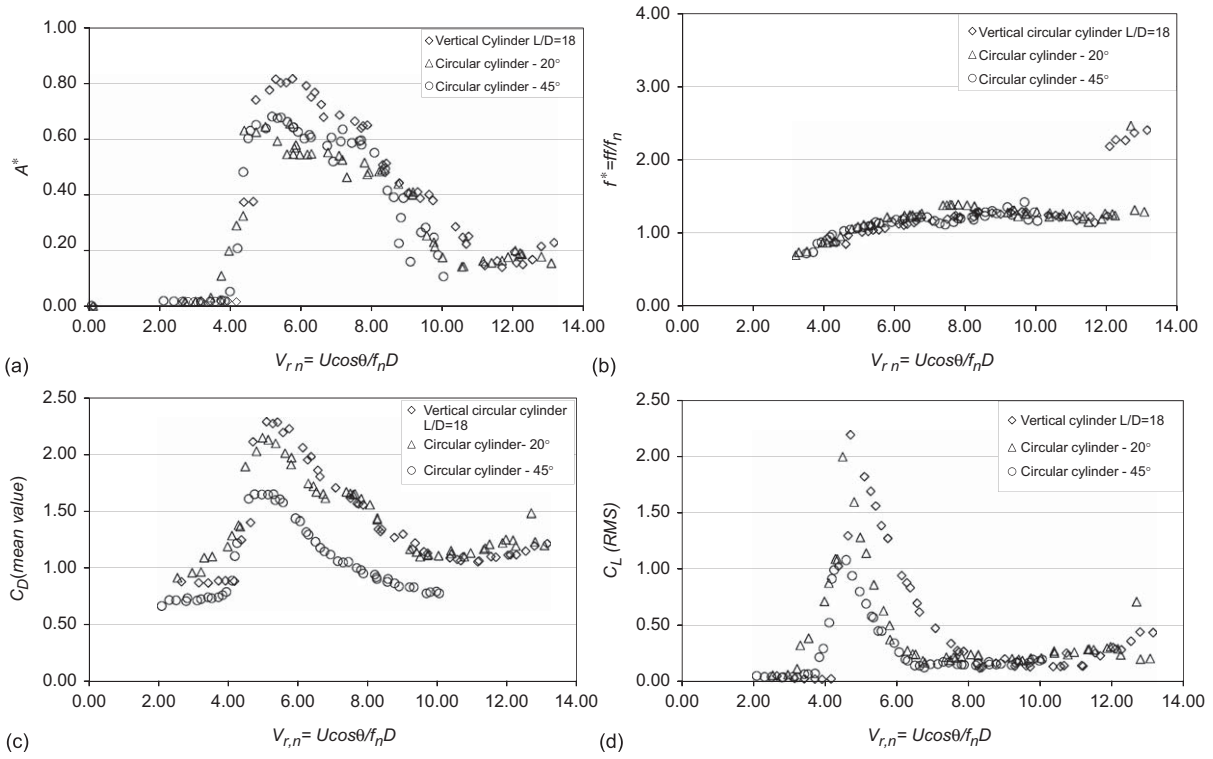

Fig. 6. Comparisons between set of experiments 1, 2, and 3. The reduced velocity is corrected by taking the projection of the free stream velocity onto the direction normal to the cylinder axis. (a) Amplitude of oscillation $A*$ versus the reduced velocity V_r; (b) frequency response through the synchronisation regime; (c) mean drag coefficient C_D through the synchronisation regime; (d) r.m.s. of lift coefficient $C_{L_{\text{rms}}}$ through the synchronisation regime.

measured in the inclined cylinder cases. In the initial branch of oscillation ($3.5 \lesssim V_{r,n} \lesssim 4.5$), the response amplitudes are very similar for all inclinations. The amplitudes of oscillation of the inclined circular cylinders are comparable, but slightly lower than, to the amplitudes observed in the vertical cylinder experiments. Furthermore, the maximum amplitude of oscillation occurs in the same range of reduced velocity, if the latter is evaluated with the velocity component normal to the cylinder axis.

Comparing the frequency response (Fig. 6(b)), the agreement is also noticeable for all inclinations. Moreover, both the lift (Fig. 6(d)) and drag (Fig. 6(c)) coefficients decrease as the inclination increases, as expected. However, if the lift coefficient is evaluated with the normal velocity ($C_L = 2F_L/\rho(U\cos\theta)^2 LD$), the values of C_L for all inclinations follow a similar behaviour in the range of reduced velocity tested, as one can see in Fig. 7.

The comparison between the circular cylinder case with $\theta = 45^\circ$ and the elliptical model shows that the last one has not depicted a defined upper-branch. In the elliptical model, the branch with the highest amplitudes corresponded approximately to the same amplitudes found in the lower branch of the vertical circular cylinder case.

In order to carry out a more detailed study of the lift force, the added mass m_a was evaluated. The added mass, m_a, defined as the term of the lift force in phase with the acceleration of the cylinder. Then, this paper does not consider the added mass using the potential approach. The lift force was decomposed using the following equation:

$$F_L(t) = -m_a\ddot{y} - c_v\dot{y}, \tag{2}$$

where c_v is the hydrodynamic damping coefficient.

Using the frequency domain described in Fujarra and Pesce (2002), we obtained the added mass coefficient, $C_a = 4m_a/\rho\pi D^2 L$. The plot of C_a versus $Vr_{r,n}$ are show for all cases tested in Fig. 8. C_a for the vertical cylinder case has a zero-crossing at about $V_{r,n} \approx 8$, and an asymptotic value $C_a \to -1$, as $V_{r,n}$ increases. This result is in agreement with those published by Vikestad et al. (2000).

In the interval $4 < V_{r,n} < 6$, the added mass coefficient is similar for both inclined cylinder cases ($\theta = 20^\circ$ and 45°). However, the elliptical model has typical values of C_a higher than those found in the circular cylinder cases,

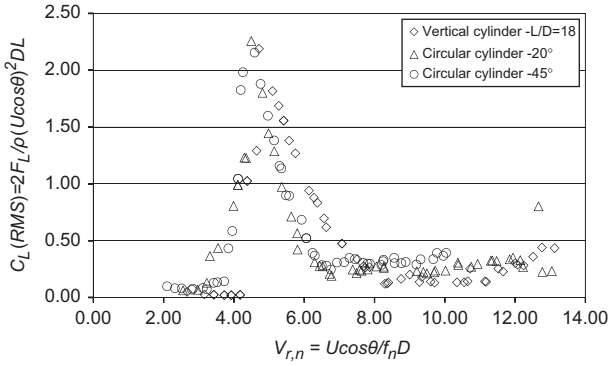

Fig. 7. Lift coefficient evaluated with the component of the free-stream normal to the cylinder axis.

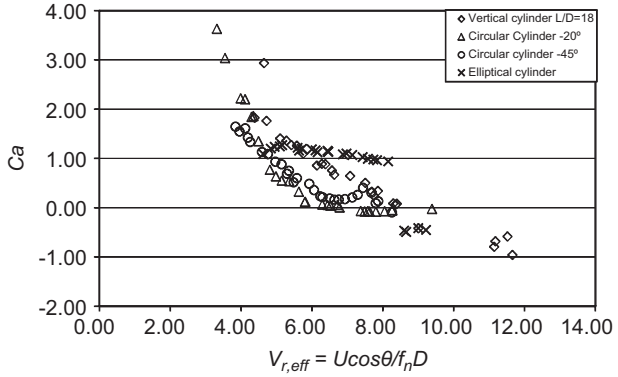

Fig. 8. Added mass coefficient plot versus corrected reduced velocity.

independently of the inclination of the later. This behaviour can be explained considering the fact that the elliptical cylinder has its bigger axis aligned with the flow direction, which implies a higher added mass in the cross flow direction.

5. Conclusion

The results for inclined circular cylinders mounted on an elastic base were found to be partially similar to the results of a vertical cylinder oscillating in the transverse direction. The reduced velocity range, in which the upper and lower branch of VIV occurs, is similar to the vertical cylinder case if the proper projected velocity is considered for the determination of reduced velocity. The amplitudes of oscillation of the inclined cylinders are comparable, but slightly lower than, to the amplitudes observed in the vertical cylinder experiments. The response amplitudes are very similar for all inclinations in the initial branch of oscillation. The maximum amplitude of oscillations of the inclined cylinder cases occur in the same range of reduced velocity. There is an agreement in frequency response as well. Moreover, both the lift and drag coefficients decrease as the inclination increases, as expected. However, if the lift coefficient is evaluated with the normal velocity, the values of C_L for all inclinations follow a similar behaviour in the range of reduced velocity tested.

The results with an elliptical cylinder oscillating in the transverse direction were found to have a different behaviour. The amplitudes of oscillation are considerably lower than those observed for a circular cylinder. This difference can be explained by the higher added mass of the elliptical cylinder. The experiments shown in this paper are part of an ongoing research project. Further work will include higher inclination angles, two-degree of freedom experiments, and PIV measurements.

Acknowledgement

We would like to acknowledge the financial support by FINEP, CNPq, and Petrobras. G.R.F and I.K. would like to acknowledge Fapesp for the scholarships that were provided during the development of this work. G.R.F is also

grateful to the Department of Naval Architecture and Ocean Engineering at USP for supporting his participation on BBVIV5 Conference. All the experimental resources were provided by NDF.

References

Assi, G.R.S., Meneghini, J.R., Aranha, J.A.P., Bearman, P.W., Casaprima, E., 2006. Experimental investigation of flow-induced vibration interference between two circular cylinders. Journal of Fluids and Structures 22, 819–827.

Bearman, P.W., 1984. Vortex shedding from oscillating bluff bodies. Annual Review of Fluid Mechanics 16, 195–222.

Fujarra, A., Pesce, C., 2002. Experiments on VIV added mass with elastically mounted cylinder in water. In: Proceedings of OMAE 02, 21th International Conference on Offshore Mechanics and Arctic Engineering.

Govardhan, R.N., Williamson, C.H.K., 2006. Defining the 'modified Griffin plot' in vortex-induced vibration: revealing the effect of Reynolds number using controlled damping. Journal of Fluids Mechanics 561, 147–180.

Khalak, A., Williamson, C.H.K., 1999. Motions, forces and modes transitions in vortex-induced vibration at low Reynolds number. Journal of Fluids and Structures 13, 813–851.

Meneghini, J.R., Saltara, F., Fregonesi, R.A., Yamamoto, C.T., Casaprima, E., Ferrari, J.J., 2004. Numerical simulations of VIV on long flexible cylinders immersed in complex flow fields. European Journal of Mechanics 23, 51–63.

Miliou, A., Vecchi, A.D., Sherwin, S.J., Graham, J.M.R., 2007. Wake dynamics of external flow past a curved circular cylinder with the free stream aligned with the plane of curvature. Journal of Fluid Mechanics 592, 89–115.

Parkinson, G., 1989. Phenomena and modelling of flow-induced vibration of bluff bodies. Progress in Aerospace Sciences 26, 169–224.

Ramberg, S., 1983. The effects of yaw and finite length upon vortex wakes of stationary and vibrating circular cylinders. Journal of Fluid Mechanics 128, 81–107.

Sarpkaya, T., 1979. Vortex-induced oscillations. Journal of Applied Mechanics 46, 241–258.

Vikestad, K., Vandiver, J.K., Larsen, C.M., 2000. Addes mass and oscillation frequency for a circular cylinder subjected to vortex-induced vibrations and external disturbances. Journal of Fluids and Structures 14, 1071–1088.

Williamson, C.H.K., Govardhan, R.N., 2004. Vortex-induced vibrations. Annual Review of Fluid Mechanics 36, 413–455.

Yamamoto, C.T., Meneghini, J.R., Saltara, F., Fregonesi, R.A., Ferrari, J.J., 2004. Numerical simulations of vortex-induced vibration on flexible cylinders. Journal of Fluids and Structures 19, 467–489.

Yttervik, R., Larsen, C., Furnes, G., 2003. Fatigue from vortex-induced vibrations of free span pipelines using statistics of current speed and direction. In: Proceedings of OMAE 03, 22nd International Conference on Offshore Mechanics and Arctic Engineering.